IMPACT OF CAPILLARY FORCES ON RESIDUAL OIL SATURATION AND FLOODING EXPERIMENTS FOR MIXED TO OIL-WET CARBONATE RESERVOIRS

Shehadeh K. Masalmeh, Shell Technology Oman

This paper was prepared for presentation at the International Symposium of the Society of Core Analysts held in Aberdeen, Scotland, UK, August 27th - 30st, 2012

1. ABSTRACT

An accurate determination of residual oil saturation (S_{orw}) has significant importance for managing ongoing waterflooding and the evaluation of the potential for tertiary EOR options. Oil trapping during immiscible displacement in porous medium is caused by capillary forces acting within the pore network. The trapped oil can be mobilized once viscous or gravity forces acting on the trapped phase exceeds the capillary forces. Numerous experiments have been conducted and reported in the past to correlate capillary or Bond number with S_{orw}. Most of the measurements have been performed on strongly water-wet porous media i.e, sand packs, outcrop or reservoir sandstone samples. For water-wet rock, S_{orw} is very well defined and insensitive to flooding rate and the critical capillary or Bond number required for mobilization of S_{orw} is in the order of 10^{-5}.

Relatively little data is available in the literature for carbonate rock and non-water-wet porous media. For non-water-wet systems, experimental artefacts due to the interference of relative permeability and capillary pressure (capillary end effect) may lead to remaining oil saturation (ROS) that is more than 15 saturation units higher than the true S_{orw}. Consequently, the waterflood recovery factor can be underestimated while the target oil for tertiary EOR processes is overestimated. It also leads to underestimation of the critical capillary or Bond number required to mobilize S_{orw} and a poor design of the EOR process.

This study is focused on the measurement of S_{orw} in carbonate reservoir samples from different rock types. For carbonates, the combination of wettability, wide pore size distribution and heterogeneity, adds to the complexity of determining S_{orw} and magnifies the experimental artefacts. The main conclusions of the study are:

1- Capillary end effect can dominate the results of the experiments (especially on short plugs) performed at reservoir rates of around 1 ft/d which leads to significant overestimation of S_{orw} and suppression of water permeability end point;
2- The relative contribution of capillary end effect increases as the permeability increases especially for heterogeneous carbonate rocks;
3- The critical capillary or Bond number of non-water-wet carbonates is much higher than those reported in the literature for water-wet sandstone; thus experiments can be performed at higher rates than those expected in the field without de-saturation of S_{orw}.
4- Once equilibrium between capillary and viscous (or gravity) forces is established, the remaining oil saturation is independent of the number of pore volumes injected.

2. INTRODUCTION

Capillary forces acting within the pore network are responsible for trapping oil during immiscible displacement. This trapped oil can be mobilized and recovered, once viscous or gravity forces acting on the trapped phase exceeds the capillary forces. The degree of recovery of residual oil by reduction of capillary forces depends upon how small they become relative to the viscous and/or gravity forces. The ratio of viscous to capillary forces is the capillary number while the ratio of gravity to capillary forces is the Bond number. Numerous experiments have been conducted and reported in the literature to correlate capillary or Bond number with S_{orw}. The main objectives of these studies are to determine S_{orw}, the critical capillary or Bond number above which the residual oil will be remobilized and the desaturation curves as a function of capillary or Bond number. Most of the measurements reported in the literature have been performed on strongly water-wet porous media i.e, sand packs, outcrop or reservoir sandstone samples.

A wide range of critical capillary or Bond number has been reported in the literature which ranges between 10^{-5} to 10^{-2}, see [4, 12] and references therein. In some cases a critical capillary number of 10^{-7} was reported while others could not detect any critical capillary number for some carbonate rocks [1, 6]. The reasons for this wide range in the reported critical capillary number are not well understood. It was already recognized that the rock wettability could be one of the reasons. For water-wet rock, S_{orw} is very well defined and insensitive to flooding rate and the critical capillary or Bond number required for mobilization of S_{orw} is in the order of 10^{-5}. The critical capillary or Bond number increases for oil-wet rocks which may partly explain the literature data. Moreover, experimental artefacts such as capillary end effect especially for non-water wet rock, could also be one of the reasons for the wide range in the reported critical capillary or Bond number.

A general problem in the measurement of fluid flow properties is that one has to ensure that the results obtained in the laboratory are representative for the field. Therefore, flooding experiments are often performed at field rate of ~1 ft/day assuming the results are more representative for the reservoir. It is difficult to attain residual oil saturations in the laboratory flooding experiments. In most of the experiments only remaining oil saturation is reached, due to the capillary end-effect or due to an extremely small mobility (very low relative permeability) of the oil phase as it approaches residual saturation. These experimental artefacts are magnified for experiments performed at low rates i.e., field rates. In many of the cases reported in the literature, remaining rather than residual oil saturation has been measured due to the experimental artefacts. Thus the measured “residual” oil saturation is too high, and it can be more than 15 saturation units higher than true S_{orw}. These experimental artefacts also lead to erroneous determination of the critical capillary or Bond number or makes it difficult to detect them. More oil will be produced as the viscous or gravity forces are increased (overcome capillary end effect) which may erroneously be interpreted as remobilization of residual oil saturation.

Relatively little data is available in the literature for carbonate rocks and non-water-wet porous media. In this paper we will present a case study of a carbonate reservoir, where the rock wettability was well characterized by a combination of spontaneous imbibition and

capillary pressure curves. The experiments were performed using both centrifuge and flooding techniques over a wide range of capillary or Bond numbers. Special attention has been given to the capillary end effect and the balance between capillary forces on one hand and viscous or gravity forces on the other hand.

3. CAPILLARY AND BOND NUMBERS

Multi-phase flow in porous media is governed by the interplay between capillary, viscous and gravitational forces. The flow regime can be characterised by the dimensionless capillary number N_c and the Bond number N_b. These numbers measure the ratio of viscous and capillary or gravitational and capillary forces at the pore scale, respectively.

A number of different, although more or less equivalent, definitions of the capillary and Bond numbers have been proposed by various researchers, see [2] and references therein. In this study the following formula for the capillary number is used:

$$N_c = \frac{v\mu}{\sigma\cos\theta} = \frac{u\mu}{\varphi\sigma\cos\theta} \quad (1)$$

where v is the interstitial velocity, u is Darcy velocity, μ is the viscosity of the displacing phase, σ is the interfacial tension, θ is the contact angle and φ is the porosity in fraction.

The Bond number measures the relative strength of gravity and capillary forces as described by eq. 2,

$$N_b = \frac{K\Delta\rho g}{\varphi\sigma\cos\theta} \quad (2)$$

where $\Delta\rho$ is the density difference between the displacing and displaced phase, g is the acceleration due to gravity and K is the absolute permeability.

A simple example is presented to highlight the problem of running laboratory experiments at field rate. The velocity of water advancement during waterflooding is in the order of 1 ft/day which is equivalent to ~ 3.5×10^{-6} m/s. Using equation 1 and assuming the interfacial tension (IFT) is 27 mN/m, water viscosity is 0.4 mPa.s (at reservoir conditions of the reservoir under study) and for simplification the contact angle is set as 0 then the capillary number is ~5×10^{-8}. To perform a laboratory flooding experiment at the same capillary number for a core sample of 1.5 inch (3.8 cm) diameter and a porosity of 0.25, the flooding rate is ~ 0.05 cm^3/minute. The expected pressure drop during such an experiment for a sample of 5 cm long, permeability of 5 mD and a water relative permeability end point of 0.5 is ~0.06 bar.

This pressure drop is very low and it is lower than the (negative) imbibition capillary entry pressure of non-water-wet samples, see Figure 1. The Figure shows the P_c curves of 3 samples of permeability 3.5, 37.4 and 127 mD, respectively. The expected viscous pressure drop (assuming no capillary forces) for the 3 samples at 100% water fractional flow rate and assuming water relative permeability end point of 0.5 is 0.09, 0.008 and 0.002 bar, respectively. In this case the flooding experiments will be dominated by capillary end effect which leads to very high remaining oil saturation. This raises the questions whether:

1- Conducting the flooding experiments at field rate is more representative and

2- Conducting the experiments at higher rate would lead to de-saturation of S_{orw}?

As most of the work done in this paper is conducted by the centrifuge, the centrifuge speed that leads to a Bond number of $5x10^{-8}$ (750 rpm) would lead to a gravity head of ~ 0.1 bar which is almost the same order of magnitude as the entry capillary pressure for the non-water-wet samples used in this study, see Figure 1. The following assumptions have been used in the calculation: plug permeability is 5 mD, density difference is 200 kg/m^3, centrifuge arm is 15 cm, sample length is 5 cm and IFT is 27 mN/m.

To avoid the experimental artefacts discussed above, the flooding experiments should be designed such that end effects are reduced by using high viscous pressure gradients and equilibration times are chosen sufficiently long to reduce "after-flow" effects due to low relative permeabilities. Reducing the experimental artefacts is not straightforward. Therefore, a combination of proper experimental design (high rates) and numerical simulation of the experimental data is required. The use of numerical simulation to aid proper interpretation of laboratory experiments proved to be an efficient tool to minimize the impact of the experimental artefacts on the results and conclusions of the study and accurately determine residual oil saturation. Following this procedure, one could resolve inconsistencies observed between residual oil saturations determined using different experimental techniques and procedures and explain the wide range of the reported critical capillary number in the literature.

High rate flooding experiments may cause the displacement to become unstable. A thorough discussion on factors affecting the stability of the displacement front can be found in [11]. One of the conditions for the onset of instability during two phase immiscible displacement is that the mobility ratio is higher than 1 ($M= K_{rwo}\mu_o/K_{row}\mu_w>1$). In one dimensional laboratory experiments, especially for light oil, there is less potential for fingers to grow. In case there is a potential of front instability, the experiment can be designed such that the rates are increased in steps where the high rate is only applied at the end in case capillary end effect is still present.

4. EXPERIMENTAL PROCEDURE

The samples used in this study went through a comprehensive special core analysis (SCAL) program [8, 9, 10]. The program included rock characterisation, centrifuge and flooding experiments. The focus of this paper is on the capillary pressure, relative permeability and residual oil saturation measurements. In order to investigate the effect of capillary forces on relative permeability and S_{orw}, the capillary and Bond numbers have also been calculated at each flooding rate or centrifuge speed. The following procedure was followed:

1- More than 100 samples of wide range of permeability have been used in the study, the characteristics of a subset of the samples are shown in Table 1.
2- The core plugs are cleaned to water-wet status and fully saturated with brine.
3- The core samples are initialised at Swi using either the centrifuge or porous plate.
4- The plugs are aged in crude oil for four weeks to restore wettability.
5- Multispeed imbibition centrifuge experiments were performed to measure the imbibition P_c curve and S_{orw}. The Bond number was calculated for each speed.

6- Some of the samples went through multiple experiments, drainage and imbibition, with and without a surfactant. The drainage data is not discussed in this paper.
7- Flooding experiments (combination of steady state and unsteady state experiments) were performed on 16 samples (only 3 samples are shown in Table 1) to investigate the effect of capillary number on relative permeability and S_{orw}.
8- The capillary number was increased in steps by increasing the displacement velocity (flow rate). The highest capillary number achieved in the flooding experiment was ~ $2x10^{-5}$ assuming a contact angle of zero. The capillary number will increase by a factor of 3 if a contact angle of 110^o is used, see the discussion in section 5.4.
9- The Bond number was increased by either increasing the centrifuge speed and/or reducing IFT by a factor 10-20 as a result of using a surfactant in the displacing fluid.

In the centrifuge experiment, the average saturation in a core plug is recorded at a set of centrifugal speeds and then a capillary pressure vs. saturation point is calculated at each speed. The capillary pressure is then calculated using either analytical techniques [3, 5] or numerical interpretation [7]. In this paper the experimental data have been interpreted by numerical simulation using MoReS, the Shell in-house simulator. The pressure difference between the fluids results from the density difference, as in gravity driven process in the field. Therefore, the Bond number (instead of capillary number) was used to scale the centrifuge experiments.

5. RESULTS AND DISCUSSION

5.1 Bond Number and S_{orw}

Figure 2 shows the oil saturation as a function of Bond number during centrifuge experiment for two samples. The Bond number is calculated using eq. 2, where σ is 27 mN/m and θ is 0. The effect of contact angle on the results of this study will be discussed in section 5.4. The oil saturation is calculated either using the average oil saturation in the sample or by numerical interpretation which calculates the oil saturation at the inlet of the sample and account for capillary end effect. The data in the figure shows that:

1- Oil production starts only as the Bond number exceed 10^{-7}.
2- The average oil saturation in the sample decreases gently as the centrifuge speed (Bond number) increases and more oil is produced at all centrifuge speeds. Therefore, using the average oil saturation curve shown in Fig. 2 may lead to a poor definition of S_{row} and to the conclusion that there is no critical Bond number for de-saturation of S_{row}, as reported in [6].
3- The oil saturation at the inlet (not affected by capillary end effect) decreases sharply as the Bond number increases until it reaches a plateau of ~10%. This plateau value is the residual oil saturation and it is reached at a Bond number $10^{-6} < N_b < 10^{-5}$. Increasing the Bond number by more than one order of magnitude and well beyond 10^{-5} did not lead to any reduction in S_{orw}.

The data in Fig. 2, clearly shows that the average oil saturation curve suffers from capillary end effect and therefore as the speed increases the capillary end effect decreases and more oil is produced. This extra oil production is not due to remobilization of S_{orw}.

A wider range of Bond number was investigated using higher permeability samples or surfactant solution where the IFT is ~1-2 mN/m. Figs. 3 and 4 show the oil saturation as a function of Bond number (inlet saturation only) for several samples with (Fig. 4) and without (Fig. 3) surfactant. As shown in Figure 3, samples of similar permeability have similar curves (Figures 3a, 3b & 3c). Figure 3d shows samples of different permeability, which explains the spread in the data. All the data in Figure 4 is measured on low permeability samples. The following observation can be drawn from the two figures:

1- Similar to Fig. 2, no oil production is observed for a Bond number lower than 10^{-7}. This demonstrates that running laboratory experiments at Bond number similar to the one experienced in the field will hardly produce any oil.
2- The data consistently show residual oil saturation of ~10-15% for all the samples irrespective of permeability and the use of surfactant.
3- The residual oil saturation is obtained at a Bond number as low as 10^{-6} for the low permeability samples and as high as $8x10^{-5}$ for the high permeability samples.
4- For the low permeability samples used in the surfactant experiments, the Bond number is increased by more than an order of magnitude compared to the water-oil experiments and the residual oil saturation is reached at N_b~$4x10^{-6}$ to $2x10^{-5}$.
5- No residual oil de-saturation is observed up to a Bond number of ~ 10^{-3}, which is 5 orders of magnitude higher than the capillary number experienced in the field.
6- The data also demonstrates that, for the case under study, the centrifuge experiments can run at much higher Bond number without the risk of remobilizing S_{orw}.

5.2 Comparison of Bond Number Data with and without Surfactant

Most of the samples used in the surfactant experiments are of low permeability. In some cases the same sample was used first without and then with surfactant, which gives the opportunity to extend the Bond number range for either the same or similar samples. Figure 5 shows the oil saturation as a function of Bond number with and without surfactant measured on samples of similar permeability, see Table 1. The Figure shows that during oil de-saturation, the surfactant data is shifted towards higher Bond number. The residual oil saturation, ~10-15%, is obtained at lower Bond number without surfactant, and a factor of ~4 increase was required to get to S_{orw} when the surfactant was used. The data also shows that the plateau oil saturation (S_{orw}) extends over more than 2 orders of magnitude without any residual oil remobilization.

5.3 The Bond Number and Sample Permeability

As shown in eq. 2, the Bond number is proportional to the permeability of the sample. Therefore, the data in Fig. 3 shows that 1- the Bond number at which oil production starts, 2- the Bond number at which S_{orw} is obtained and 3- the maximum Bond number used in the experiment increase as the permeability increases. This triggered the question whether a better correlation could be achieved without the permeability in eq. 2. Figure 6a shows the oil saturation as a function of Bond number for 4 samples with permeability of 4.1, 13.5, 52.7 and 105.8 mD, respectively. The same data is shown in Figure 6b after dividing the

Bond number by the permeability of the samples (N_b is divided by 4.1, 13.5, 52.7 and 105.8, respectively, to keep the same scale). As shown in the figure, the data collapse into almost one curve indicating a better correlation when eq. 2 is divided by the permeability.

5.4 Effect of Wettability on the Bond Number

So far the Bond number was calculated assuming a contact angle equal to zero, i.e, strongly water-wet assumption. The wettability of the samples used in this study has been characterized by the use of capillary pressures (primary drainage, imbibition and secondary drainage P_c curves) and spontaneous imbibition of water and oil. Spontaneous imbibition data showed that hardly any oil or water has been imbibed. The capillary pressure curves have been used to calculate an apparent advanced contact angle during imbibition experiments, see [8, 9]. The calculated apparent contact angle is between 105^o-115^o, for most of the samples. Therefore, the water wet assumption underestimates the Bond number calculated in Figures 2-6. If the calculated apparent contact angle is used in eq. 2, the Bond number would increase by a factor of 2-4.

5.5 Capillary End Effect and Sample Permeability

One of the common misunderstandings in flooding experiments is that capillary end effect is more significant for low permeability plugs. Therefore, it is assumed that the data of high permeability samples is not impacted by capillary end effect or capillary forces. In reality, the capillary end effect is more dominant for high permeability samples if the same rate is used and if the samples have the same contact angle. Using bundle tube model, the permeability (K) of a homogeneous sample with uni-modal pore size distribution is:

$$K \propto \phi R^2 \tag{3}$$

From Darcy's law, the viscous pressure (ΔP_{vis}) is inversely proportional to permeability (i.e., inversely proportional to R^2) while the capillary pressure is inversely proportional to R, where R is the pore throat size.

$$\Delta P_{vis} \propto \frac{1}{K} \propto \frac{1}{R^2} \tag{4}$$

$$P_c = \frac{2\sigma \cos\theta}{R} \tag{5}$$

Therefore, as the permeability increases the viscous pressure decreases faster than capillary pressure which makes capillary forces relatively more important and leads to higher capillary end effect in flooding experiments. Moreover, high permeability samples are usually more heterogeneous and often exhibit bi-modal pore size distribution where the big pores determine the permeability and the small pores (but still filled with oil) determine the capillary pressure at low oil saturation. Therefore, for bi-modal high permeability samples, R in eq. 4 is the radius of the big throats while R in eq. 5 is radius of the small throats. This enhances the relative importance of capillary forces and increases capillary end effect for such high permeable samples. Figure 7 shows simulation of water flooding experiments for two samples of 5 and 150 mD, respectively. The capillary pressure curves used in the simulation runs are similar to those shown in Fig. 1 for the respective permeability. The simulation runs were performed at different flow rates using the same relative permeability

curves and S_{orw} for the two core samples. As demonstrated in the figure, the high permeability sample shows lower recovery at all injection rates. The difference at the lowest injection rate is ~20 saturation units.

The simulation data shows also that once equilibrium between capillary and viscous forces is established, the remaining oil saturation is independent of the number of pore volumes injected, see Fig. 7b, especially for the high permeability run. It is clear from the slope of the production curves at the low rates that oil production either completely ceases or only very small change is expected if the run continues for 100s of pore volumes. Significantly higher oil recovery is observed as the rate is increased.

The number of injected pore volumes can lead to higher recovery only for the case where viscous forces are still higher than capillary forces but the oil is produced at very low rate due to an extremely small mobility of the oil phase. This could happen either as oil saturation approaches S_{orw} (low relative permeability), or as it approaches the equilibrium between viscous and capillary forces. In both cases, long time (many pore volumes) is required to get to equilibrium, as clearly shown in Fig. 7a, especially the last step. However, in both cases, oil production will stop once equilibrium is reached and injecting many pore volumes will not overcome capillary end effect.

5.6 Experimental verification

Steady state experiments (including bump rates) have been run on 16 high and low permeable samples. The experiments were run at 30 cc/hour and 50 cc/hour for the low and high permeability samples, respectively. Then two bump rates of 200 cc/hour and 500 cc/hour were performed to overcome capillary end effect and investigate the impact of capillary number on S_{orw}. Only the data of two samples will be discussed in this section.

5.6.1 Capillary End Effect and Rock Permeability

Examples of in-situ saturation profiles of low and high permeable samples are shown in Fig. 8. Even though a higher rate was used, the high permeability sample shows much higher capillary end effect compared with the low permeability sample. Table 2 shows the capillary number, flow rate and average saturation for both samples together with S_{orw}. The residual saturation was obtained from the numerical interpretation of the data and the saturation profile at the inlet of the sample which is less influenced by end effect. The capillary number was calculated assuming a contact angle equal to zero. The values in table 2 will increase by a factor of 2-4 if the apparent contact angle of 105^{o}-115^{o} is used in eq. 1.

The base rates used in the experiments (30 and 50 cc/hour) are much higher than the field rate of 1 ft/day (~10 and ~16 ft/day, respectively). However, the capillary end effect is still significant, and as expected from the discussion in section 5.5, it is more profound in the high permeability sample. The average oil saturation is ~20 saturation units higher than S_{orw} for the high permeability sample. As the rate increased, the capillary end effect is reduced and more oil is produced. The high flooding rates used in the experiments did not lead to any de-saturation of residual oil. For example, the last two saturation profiles for the low permeability sample (200 cc/hour and 500 cc/hour) are almost the same. Moreover, in all flooding experiments (including the bump rates) both the average oil saturation and oil

saturation at the inlet are still higher than the residual oil saturation obtained from the centrifuge (at $N_b \sim 10^{-6}$), see Figs. 3&6.

5.7 Flooding Experiments at Field Rate

All the flooding experiments were run at high flow rates; no data is available for the rock used in this study using field rates. Therefore, numerical simulation was used to estimate the impact of using field rates on both relative permeability and remaining oil saturation. We have followed the following procedure:

1- History match the high rate experiments to obtain the oil and water relative permeability curves. A history matched example using one of the samples is presented in [10].
2- Re-run the simulation deck at field rate (~0.05 cc/minute) using the estimated relative permeability and P_c curves obtained from history matching of the high rate experiments and the centrifuge data. To facilitate comparison with the available data, the simulation run is performed to mimic a steady state experiment.
3- Use pressure drop and production data to estimate the relative permeability curves and residual oil saturation assuming zero capillary pressure. In this study, the discussion is limited to S_{orw} and the water relative permeability end point K_{rwo}.

The results of the simulation runs for both a high and low permeability samples are shown in Figures 9&10. Figure 9 shows the production data as a function of time for the high rate experiment and low rate simulation run for low and high permeability samples (see Figs. 9a & 9b). As shown in the figure, for the high permeability sample a significant difference in the oil saturation is evident for most of the fractional flow rates apart from the bump rates. The oil saturation at 100% water fractional flow rate is 50% and 34% for the low and high rate runs, respectively. This oil saturation achieved in the low rate simulation run (before the bump rates) is more than 30 saturation units higher than S_{orw}, see the data in Table 2. For the low permeability sample, the impact of capillary end effect is less significant, especially when both oil and water fractional flow rates are high (see the data between 70 and 160 hours). However, the remaining oil saturation at the 30 cc/hour is ~ 20 saturation units higher than S_{orw}.

Figure 10 shows the saturation profiles of the high and low rate runs of the high permeable sample. The last two saturation profiles (Sat10 and Sat11) are the same as they correspond to the same bump rates used in both runs. Significant difference is evident between the corresponding saturation profiles (same fractional flow but different total rate). For the low rate saturation profiles (Fig. 10a), the capillary end effect is evident at all fractional flow rates, see the inhomogeneous saturation profiles (Sat2 to Sat9). For the higher rate run (30 cc/hour), the capillary end effect is only clear for the 100% water fractional flow step (Sat9). The capillary end effect is still clear even at the high bump rates (200 cc/hour and 500 cc/hour), Sat10 and Sat11.

To illustrate the impact of capillary end effect on the conventional calculation of relative permeability, the pressure and flow rate during the high and low rate simulation runs were used to calculate water relative permeability end point (K_{rwo}). Using Darcy's law, the end point at low rate is:

$$K_{rwo}^{LR} = \frac{\Delta P_{HR}}{\Delta P_{LR}} \frac{q_{LR}}{q_{HR}} K_{rwo}^{HR} \quad (6)$$

For the high permeability sample (4_17), the viscous pressure is 0.03 and 0.068 bar for the low and high rate simulation runs and the flow rates are 3 and 50 cm^3/hour, respectively. Substituting these numbers in eq. 10, we get K_{rwo}^{LR} =0.135 K_{rwo}^{HR}. However, the saturation at which the water relative permeability end points are calculated is markedly different due to the end effect (50% and 66%). The pressure drop and flow rate that coincide with the same water saturation in the high rate run were used in eq. 6 and the low rate end point increased to K_{rwo}^{LR} =0.5 K_{rwo}^{HR}. This shows that the error in K_{rwo} can be anywhere between a factor 2 to 8 depending on whether the saturation difference is taken into account or not.

As evident from Figs. 9&10, capillary end effect dominates the data of the low rate run apart from the bump rates. Running such an experiment at field rate in the laboratory will lead to significant errors in the results, both the residual oil saturation and the relative permeability curves. The experimental data cannot be reconciled by numerical simulation especially if no bump rates are used at the end of the experiment.

6. CONCLUSIONS

In this paper we have investigated the impact of capillary forces and capillary end effect on residual oil saturation, relative permeability and laboratory flooding experimental data for a non-water-wet carbonate rock. The main conclusions of the study are:

1- For the reservoir under study, the residual oil saturation is well defined, ~10-15%.
2- Performing the flooding experiments at reservoir rates of ~1 ft/d will lead to much higher remaining oil saturation as the data is dominated by capillary end effect.
3- The residual oil saturation was obtained at Bond number of 10^{-6} or higher, increasing the Bond number by more than 2-3 orders of magnitude did not lead to any remobilization of the trapped oil. Thus experiments can be performed at higher rates than those expected in the field without the risk of de-saturation of S_{orw}.
4- The relative contribution of capillary end effect increases as the permeability increases especially for heterogeneous carbonate rocks.
5- The data shows no correlation between S_{orw} and rock permeability. This conclusion cannot be generalized and need to be checked for other rock and fluid systems.
6- The critical capillary or Bond number of non-water-wet carbonates is much higher than those reported in the literature for water-wet sandstone.
7- The low rate experiments also lead to erroneous relative permeability curves, a factor of 2 underestimation in the water end point (K_{rwo}) can be easily observed.
8- Once an equilibrium between capillary and viscous (or gravity) forces is established, the remaining oil saturation is independent of the number of pore volumes injected.

The data presented in this paper has significant impact on the design of any subsequent EOR process. Laboratory core flooding tests are often used to measure S_{orw}. The same core samples are then usually subjected to EOR flooding experiments to estimate the extra amount of oil that can be recovered with the specific EOR option. Proper assessment of the EOR target should take into account the capillary end effect on S_{orw} derived from laboratory experiments. Failure to accurately determine S_{orw} will lead to wrong estimates of the recovery factor of waterflooding and overestimates the potential target for the subsequent EOR methods. For example flooding with surfactant solution after waterflood will reduce capillary pressure and may lead to significant extra oil production by reducing capillary end effect which is not necessarily observed in the reservoir. The current study also shows that for non-water wet rock, surfactant flooding will require much higher reduction in the IFT to mobilize residual oil saturation than for water-wet rocks. No trapped oil remobilization was observed up to a Bond number of 10^{-3} which is almost 5 orders of magnitude higher than the capillary number experienced in the field.

REFERENCES

1- Abrams, A.: "The influence of fluid viscosity, interfacial tension, and flow velocity on residual oil saturation left by waterflood" SPEJ (October 1975), 437–447.
2- Cense, A.W. and Berg, S.: "The viscous-capillary paradox in 2-phase flow in porous media", SCA 2009-13, Noordwijk aan Zee, The Netherlands 27-30 September, (2009).
3- Forbes, P.: "Centrifuge Data Analysis Techniques: An SCA Survey on the Calculation of Drainage Capillary Pressure Curves from Centrifuge Measurements", SCA 9714, Calgary, Canada (1997).
4- Fulcher, R.A., Ertekin, T., Stahl, C.D.:"Effect of Capillary Number and its Constituents on Two-Phase Relative Permeability Curves", JPT, (Feb 1985), p 249.
5- Hassler, G. & Brunner, E.: "Measurements of capillary pressure in small core samples", Transactions AIME (1954) 160, 114–123.
6- Kamath, J., Meyer, R.F., Nakagawa, F,M.: "Understanding Waterflood Residual Oil Saturation of Four Carbonate Rock Types", SPE 71505, SPE Annual Technical Conference and Exhibition, New Orleans, 30 September–3 October (2001).
7- Maas, J.G. and Schulte A.M.: "Computer Simulation of Special Core Analysis (SCAL) Flow Experiments Shared on the Internet", SCA-9719, Calgary, (1997).
8- Masalmeh, S.K. and Jing, X.D. "Capillary Pressure Characteristics of Carbonate Reservoirs: Relationship between Drainage and Imbibition Curves", SCA 2006-16, Trondheim, Norway, 12-16 September, (2006).
9- Masalmeh, S.K. and Jing, X.D.: "Improved Characterisation and Modelling of Carbonate Reservoirs for Predicting Waterflooding Performance", SPE paper 11722_PP, IPTC conference held in Dubai, U.A.E., 4–6 December (2007).
10- Masalmeh, S.K. and Jing, X.D.: 'The Importance of Special Core Analysis in Modelling Remaining Oil Saturation in Carbonate Fields', SCA 2008-3, Abu Dhabi, October (2008).

11- Peters, E.J. and Flock, D.L.: "The Onset of Instability During Two-Phase Immiscible Displacement in Porous Media"; SPE Journal, 249 – 258, April 1981.
12- Sheng, James J.: "Modern Chemical Enhanced Oil Recovery: Theory and Practice", Elsevier, USA, (2011), p 293-314.

Table 1: Characteristics of the samples used in the experimental program

id	Swc	Sor	K_brine	Phi%
15a	0.1	0.15	15.2	0.289
16b	0.12	0.1	37.4	0.31
19b	0.19	0.1	13.5	0.27
20b	0.1	0.1	3.1	0.23
20c	0.1	0.1	3.1	0.21
22a	0.1	0.1	13.6	0.25
27b	0.11	0.1	52.7	0.31
28b	0.1	0.1	19.7	0.30
s31b	0.15	0.1	105.8	0.28
47b	0.24	0.11	5.4	0.28
2_3b	0.19	0.11	8.5	0.26
2_3c	0.12	0.12	7.1	0.25
2_4	0.09	0.1	13.5	0.27
2_7b	0.12	0.1	18.4	0.31
2_8	0.12	0.12	14.7	0.31
2_14	0.07	0.1	3.5	0.28
2_17	0.12	0.11	5.9	0.23
2_18	0.14	0.1	1.4	0.2
2_22	0.15	0.11	2.5	0.26
3_14	0.29	0.12	77.5	0.2
3_15	0.18	0.08	49.4	0.25
3_21	0.11	0.1	7.3	0.27
3_26	0.11	0.09	4.1	0.28

id	Swc	Sor	K_brine	Phi%
Samples Used in Flooding Experiments				
3_42	0.08	0.13	4.1	0.29
4_16	0.09	0.13	127	0.30
4_17	0.07	0.15	210	0.27
Plugs used in surfactant experiments				
2_23s	0.11	0.08	2.6	0.26
2_24s	0.07	0.08	3.4	0.27
3_20s	0	0.1	4.9	0.29
3_23s	0.65	0.09	3.3	0.26
3_25s	0	0.12	5.1	0.3
3_32s	0.08	0.13	2.4	0.29
3_36s	0.09	0.11	2.6	0.3
3_39s	0.48	0.14	4.4	0.28
3_46s	0.48	0.14	4.4	0.28

Table 2: Capillary Number, flow rates, water saturation and S_{orw} for two samples used in flooding experiments.

Rate	N_c	3_42 (Low perm)		4_17 (High Perm)	
		Sw (average)	Sorw	Sw (average)	Sorw
30	$7.2 X10^{-7}$	0.74	0.15		0.13
50	$1.2X10^{-6}$			0.66	
200	$4.8X10^{-6}$	0.80		0.73	
500	$1.2X10^{-5}$	0.83		0.78	

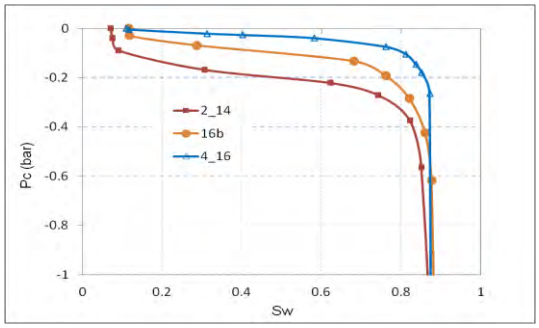

Figure 1: Capillary Pressure curves of 3 samples of different permeabilities, see table 1.

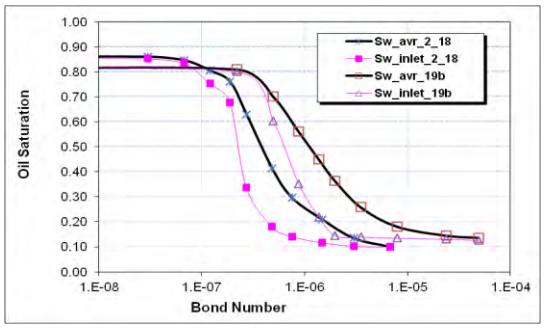

Figure 2: Oil saturation as a function of bond number during centrifuge experiment for two samples

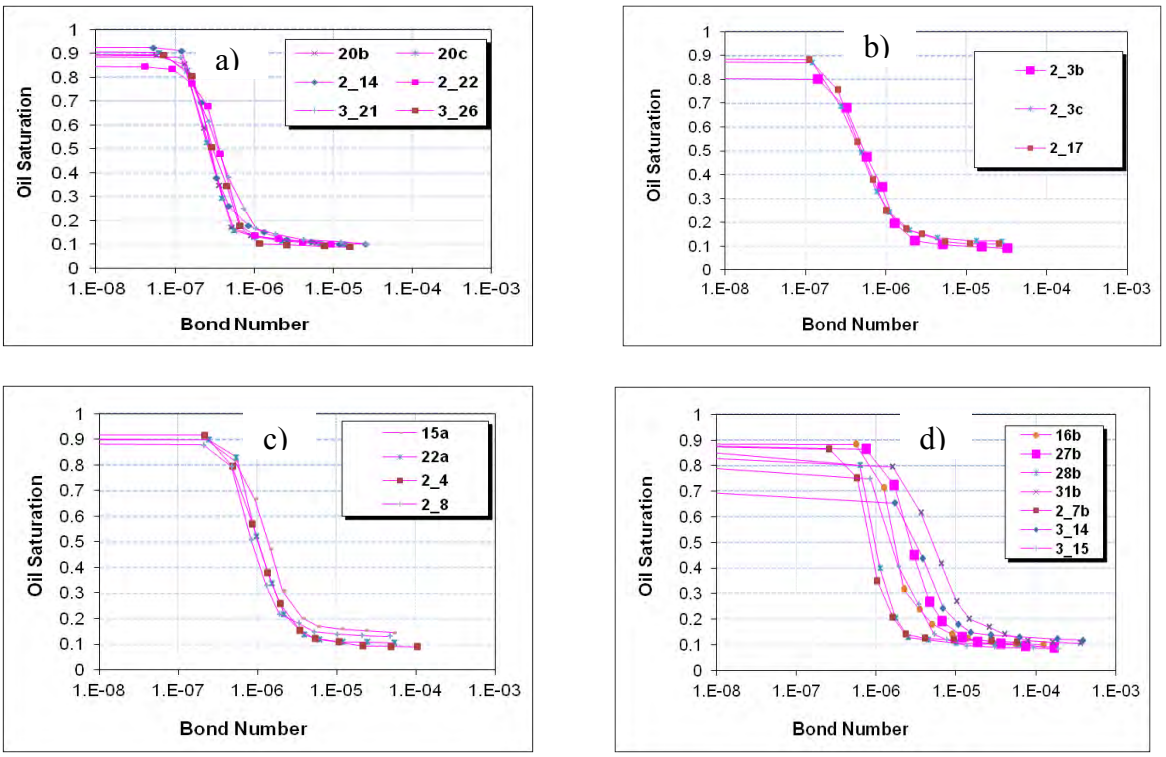

Figure 3: Oil saturation as a function of bond number for samples of different permeabilities.

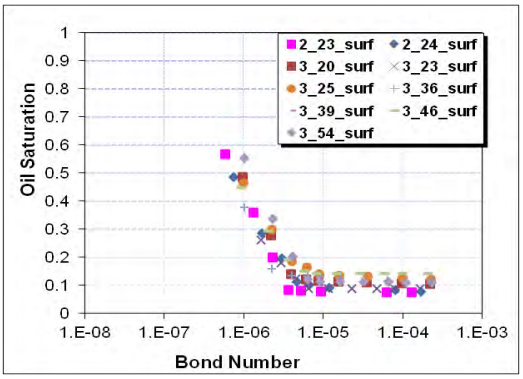

Figure 4: Oil saturation vs. bond number for different samples using surfactant.

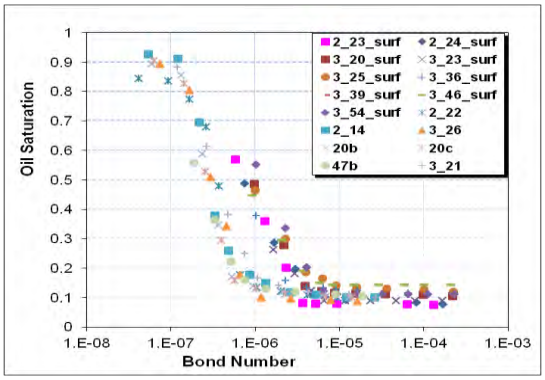

Figure 5: Oil saturation vs. bond number for samples of similar permeability, with and without surfactant.

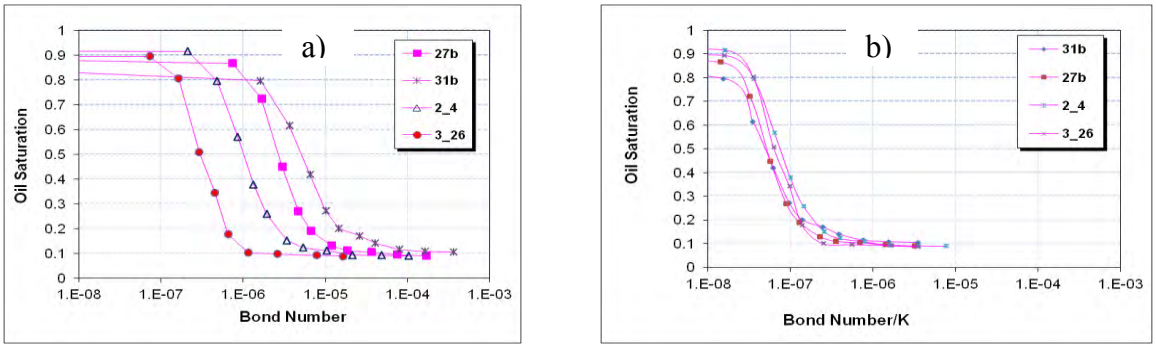

Figure 6: Oil saturation vs bond number a) Bond number calculated using eq. 2 and b) Bond number is divided by the permeability, see text.

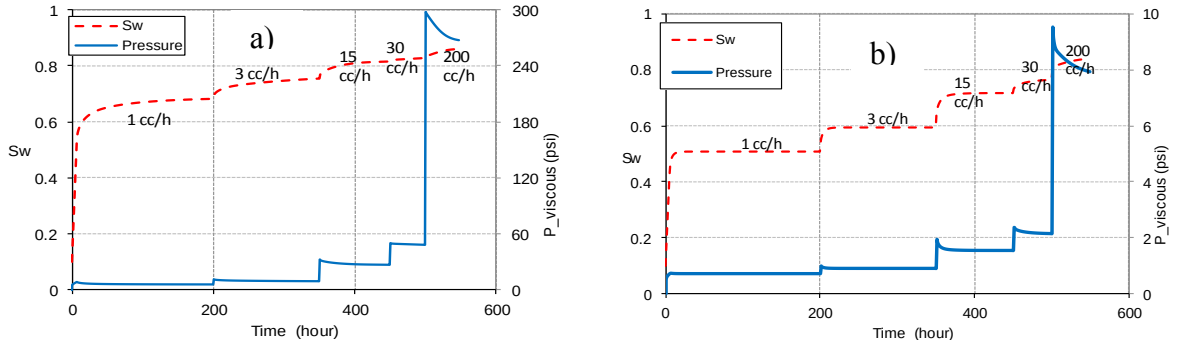

Figure 7: Simulation data showing capillary end effect: a) low permeability and b) high permeability samples.

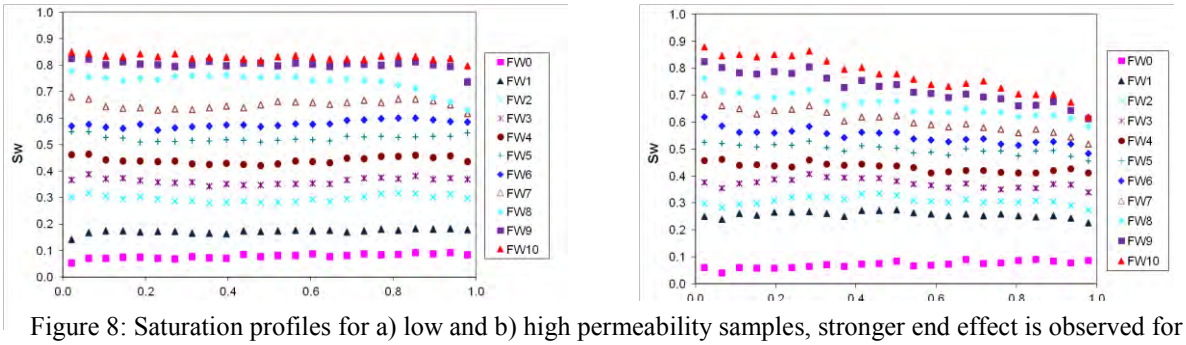

Figure 8: Saturation profiles for a) low and b) high permeability samples, stronger end effect is observed for high permeability

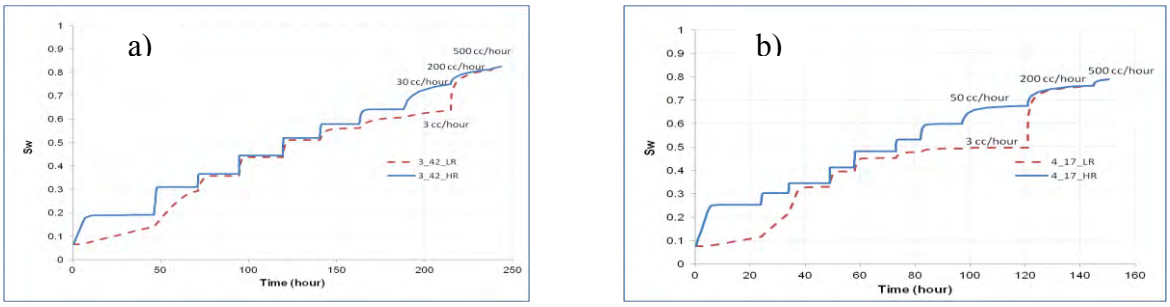

Figure 9: Comparison of the experimental data (high rate) and simulation data (low rate) for a) low and b) high permeability samples

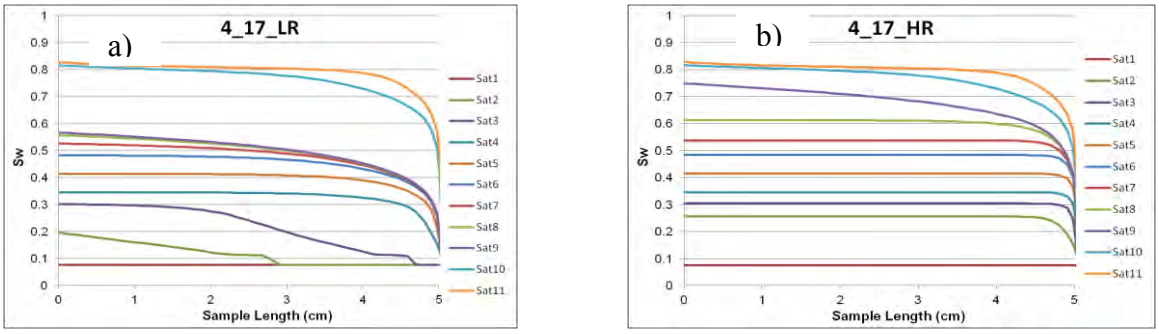

Figure 10: Saturation profiles of the low rate (a) and the high rate (b) for the high permeability sample